

Hard Particle Induced Physical Damage and Demagnetization in the Head-Disk Interface

Jia Zhao*⁺, Shaomin Xiong⁺ and David B. Bogy⁺

*State Key Laboratory for Mechanical Behavior of Materials, Xi'an Jiaotong University,
Xi'an, Shaanxi, 710049

⁺Computer Mechanics Laboratory, Department of Mechanical Engineering,
5146 Etcheverry Hall, University of California, Berkeley, CA 94720

Abstract

Test stand experiments were performed in which 44 μm stainless steel particles and 0.3 μm alumina particles were introduced at the head-disk interface (HDI) of hard disk drives (HDD), and their damage to the HDI was observed and evaluated. An Olympus HDI reliability tester was used to fly the sliders at different radii. Optical microscopy, atomic force microscopy (AFM) and magnetic force microscopy (MFM) were used to examine the slider's and the disk's physical and magnetic conditions after the particle experiments. Results showed that both particles were able to produce scratches and demagnetization but in very different ways. The alumina particles can become entrapped in the HDI to cause physical damage to both sliders and disks whereas the larger stainless steel particles cannot. For alumina particles, plastic deformation and high temperatures occur simultaneously to cause demagnetization when a particle induced scratch is formed. Stainless steel particles can induce high-speed slider/disk contact and physical damage to the slider's trailing edge through their contributions to flying instability.

1. INTRODUCTION

Particle induced damage is an ongoing problem in hard disc drives, and it has existed ever since the disc drive was invented. Particles cause data loss by inducing physical and magnetic damages on the disc surface [1]. Even though hard disk drives are well sealed to isolate them from particles from external surroundings, internal debris due to components wear, chipped pieces from sliders [2], residual diamond polishing abrasives [3], etc., can still be particle sources. To achieve a higher recording density, a smaller bit size and lower flying height is required, and this continues to be a primary goal of the HDD industry. However, it also makes the HDI more vulnerable to any slight disturbance that affects slider's flying stability.

When particles become entrapped in the HDI, they produce physical damage to both sliders and disks [1, 4]. Particle sizes and their physical properties are the dominant factors to determine the severity of the damage, which ranges from soft-particle smear on surfaces, embedded particles in the media, scratches on both surfaces, crater like damage sites, etc.. The particles can affect the slider's flying stability or cause a slider crash by hitting or being entrapped; for disks, particle caused scratches account for demagnetization, which results in read-back signal errors or data loss. Recently researchers have found that the reason for scratch induced demagnetization is grain tilt of the recording layer material [5]. Another cause of demagnetization is the heating

of the recording layer to its flash temperature. The heat flux can be from a high-speed slider/disk contact or soft particles-HDI interaction [6, 7]. If the width of the demagnetized zone is comparable to the width of a track a read-back signal error can occur. Since tracks are continually getting thinner and the bits are getting smaller in order to meet growing recording capacity requirements, particle caused demagnetization has become a serious problem. Former work by Zhang [1] suggested that large particles are swept away by the leading edge of a slider, and therefore they were not taken into consideration as a cause of physical damage. Furukawa used a stylus to investigate demagnetization caused by scratches, whereas Roy [8] employed soft particles to research heat induced demagnetization, but few works have studied hard particle induced demagnetization. This paper aims to introduce both small and large hard particles to test their physical damage in the HDI, and investigate demagnetization patterns they produce.

2. EXPERIMENTS

3.5" magnetic disks and pico-sliders ($1.25\text{mm} \times 1.00\text{mm} \times 0.30\text{mm}$) were employed to conduct the particle experiments, and a magnetic encoder system was used to write data as a continuous '0101' pattern as shown in Fig. 1 (from the outer radius at 1.85" to the middle radius at 1.38" of the disks.) Fig. 2 shows the magnetic encoder system, which includes a spindle, an arm equipped with a linear motor to hold a magnetic head, which is connected to a preamplifier and a circuit board to control the writing process. During the data

writing process, the disks are rotating at 1500 RPM while the magnetic head is moving radially at $3.75\mu\text{m/s}$ from the radii of $1.85''$ to $1.35''$. A 150 nm track width was obtained and the size of the magnetic bits varies from 90 nm on the outer boundary track to 70 nm on the inner boundary track.

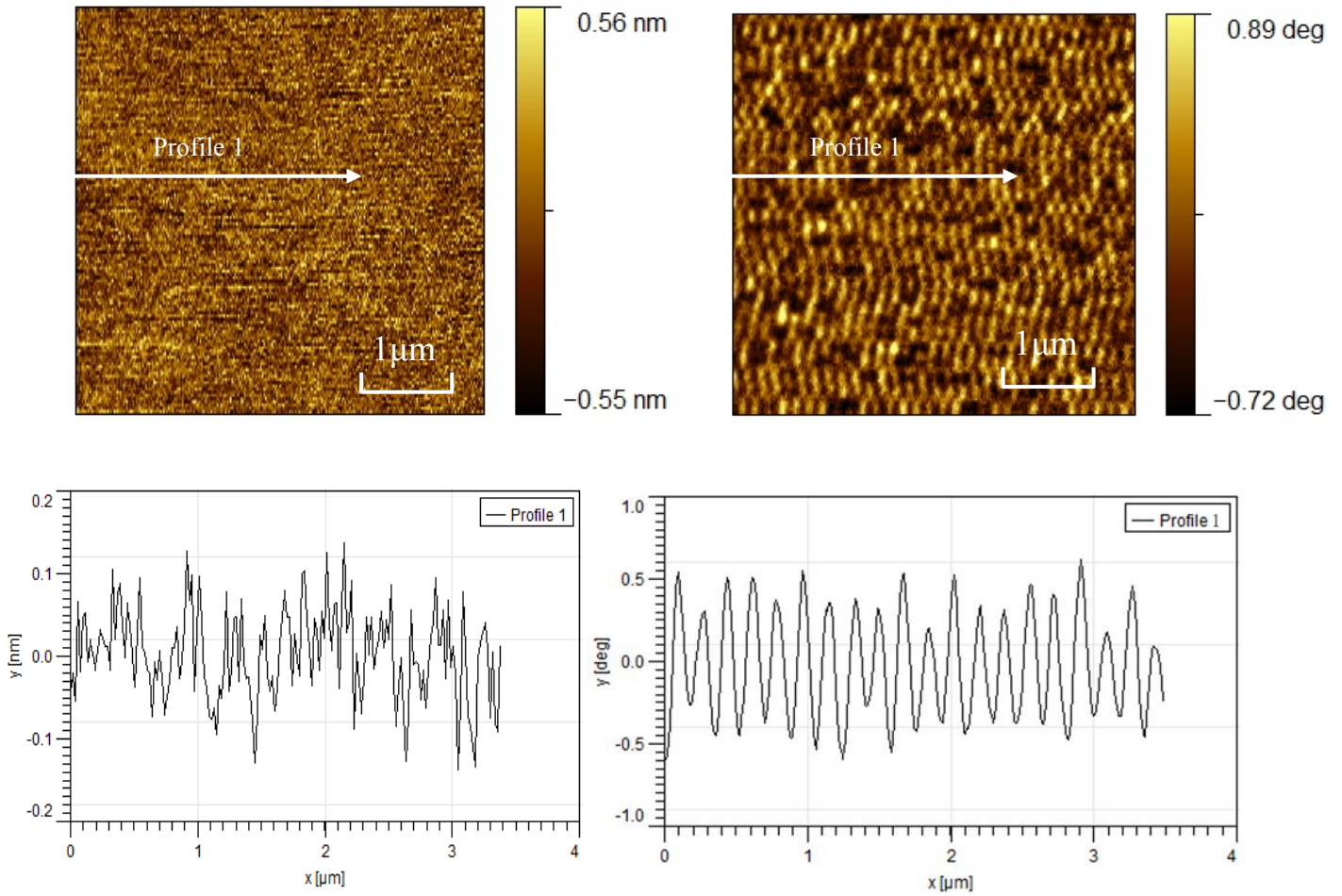


Fig.1 Initial surface profile and magnetic field distribution of data written disks

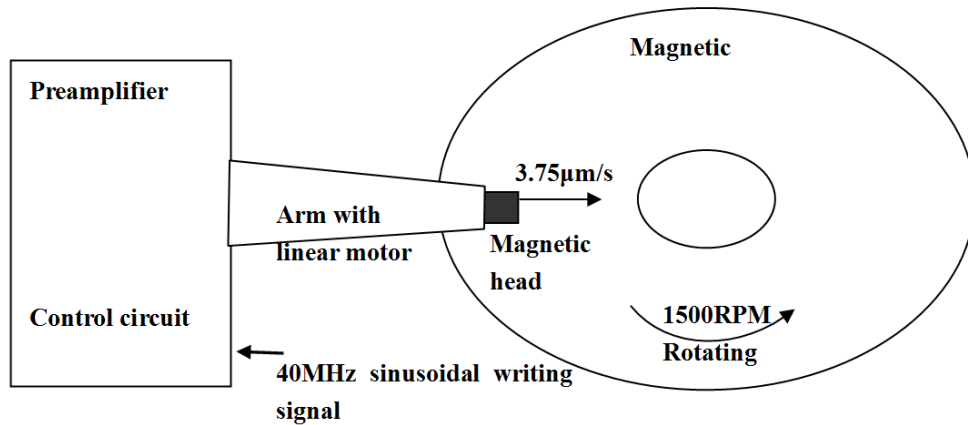


Fig.2 Schematic illustration of the magnetic encoder system

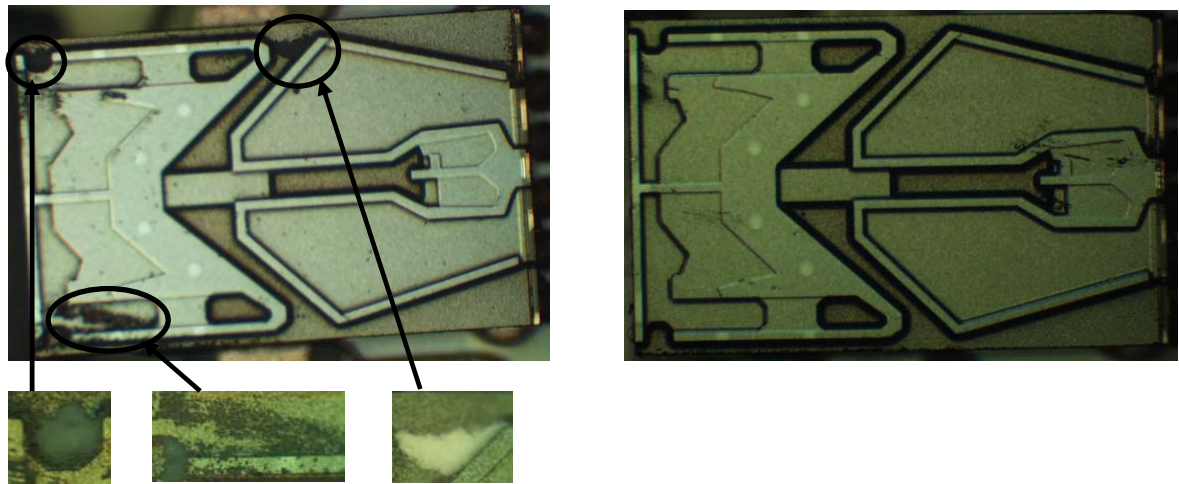
An Olympus HDI reliability tester was used to fly the sliders on the data written disks with a disk rotational speed of 5400 RPM. The time period for each experiment was 5 min. The particles were of two types, 44 μm stainless steel and 0.3 μm alumina, which were introduced uniformly by a swab smearing technique on the disk surface. After the particle experiments, an Olympus Vanox optical microscope was used to examine the slider's surface and a Digital Instruments 3100 atomic and magnetic force microscope was employed to investigate the particle-caused scratches and demagnetization on the disk surface.

3. RESULTS AND DISCUSSION

3.1 PARTICLE INDUCED SLIDER DAMAGE

Fig.3 and Fig.4 show slider profiles after the fixed radius and sweeping radii experiments with both particles. From Fig.3 (a) and Fig.4 (a) it can be seen that 0.3 μm alumina particles entered into the HDI and caused surface layer peeling and scratches to the slider surface. In the fixed radius experiment of

alumina particles as shown in Fig.3 (a), the slider's surface close to the end of the leading edge and the upper middle region was partially damaged from scratches and peeling, most of which were located in the deep etched area.



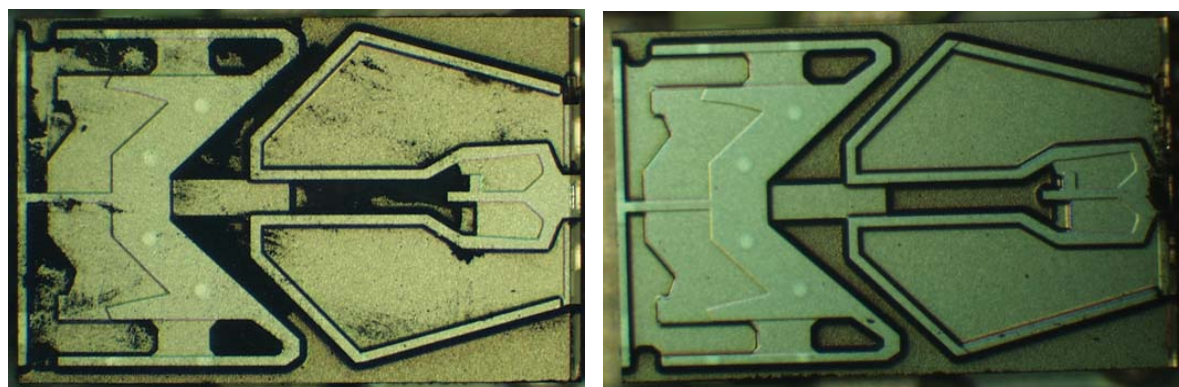
(a) 0.3 μm alumina particles

(b) 44 μm stainless steel particles

Fig.3 Slider surface profile after fixed radius experiments at radius 1.7'' on disk surface

Particle damage is seen to be more severe in the sweeping experiment

by comparing Fig. 4 (a) with Fig.3 (a), however, the transducers survived in both cases and there was no slider-disk contact.



(a) 0.3 μm alumina particles

(b) 44 μm stainless steel particles

Fig.4 Slider surface profile after sweeping experiments between radius 1.5'' and 1.0'' on disk surface

Fig.3 (b) and Fig.4 (b) show surface profiles after 44 μm stainless steel particle experiments. There were some dots and lines around the transducer in the fixed radius experiment as shown in Fig.3 (b). The transducer and its vicinity were almost completely destroyed in the sweeping experiments as shown in Fig. 4 (b). Since the stainless steel particles are too large to enter the HDI, slider-disk high-speed contact due to flying instability is the only way to account for the damage.

As seen from the slider's surface profile after the particle experiments it is clear that the particle-caused damage in the sweeping experiments is more severe for both particles. For the alumina particles, in addition to those entering the leading edge, the particles also entered the HDI from the outer and inner rails. Fig. 5 shows possible inlets of particles. Inlet A

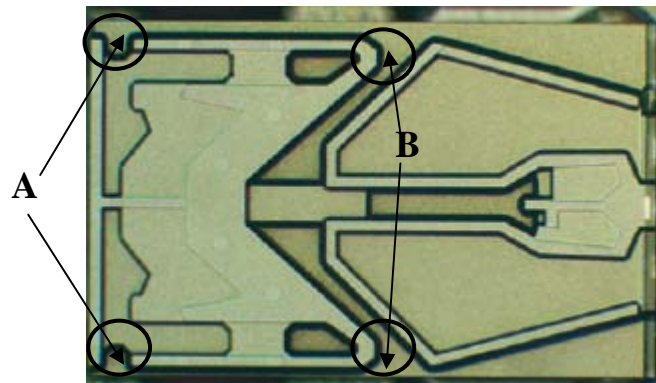


Fig.5 Possible inlets for 0.3 μm alumina particles

is around two end points of the leading edge and inlet B is in the middle of outer rail and inner rail, both of these channels have the largest recess height of the ABS design. In the fixed radius experiments, particles entered the HDI only at the leading edge, so inlet A on the leading edge acts as the main entry

location. For this specific ABS design, there is one more inlet for particles when the slider is sweeping, which is inlet B. Since inlet B is followed by long channels extending to the slider's center, the particles accumulated in the channels, becoming a potential source of particles for the HDI. The particle accumulation can be seen in Fig.4 (a), from which it can be concluded that the alumina particles enter the HDI from inlets with the largest recess height then tend to remain there and damage those areas and their vicinity. In the case of the stainless steel particle experiments, no sign of particle caused damage was detected, hence it can be surmized that the stainless steel particles cannot enter the HDI but are swept aside by the leading edge. However since $44\ \mu\text{m}$ is 4.4% of the width of a pico-slider used in this experiment, the stainless steel particles are large enough to affect the flying height. The trailing edge damages seen in Fig.3 (b) and Fig.4 (b) indicate that high speed slider-disk contact occurred during the particle experiments, and high shearing stress peeled off the brittle surface layer of the sliders. There are more possibilities for the slider to hit particles on the disk surface in the sweeping experiment because of the broader scanning area, which accounts for the larger trailing edge damage seen in Fig.4 (b).

3.2 PARTICLE INDUCED DISK DAMAGE AND DEMAGNETIZATION

Fig.6 shows that particles entrapped in the HDI are able to cause scratches and demagnetization to the disks in the fixed radius experiment. The identity of the particles in Fig.6 (a) cannot be determined by AFM. They can be either

peeled chips from the slider surface layer or disintegrated alumina particle fragments. The maximum depth of the scratches in Fig.6 (a) is 1.52 nm, and the surrounding area of the scratches on the top of the image is also demagnetized as shown in Fig.6 (b). On the bottom of Fig.6 (a), tiny pieces are found in an area without large surface height variation, but demagnetization of the area still can be seen in Fig.6 (b).

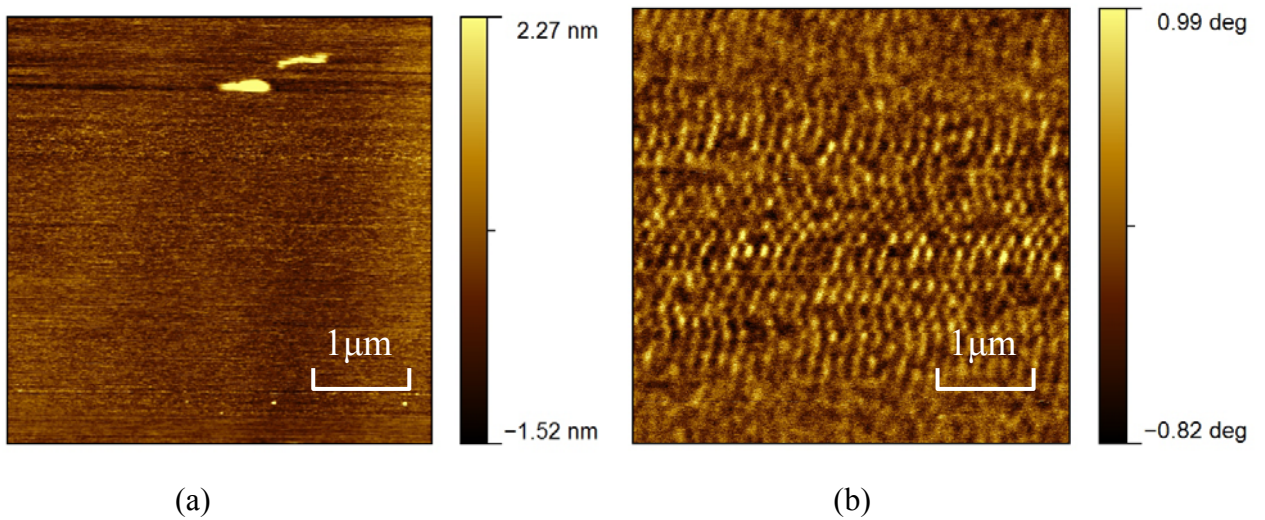


Fig.6 AFM and MFM images after fixed radius experiments of 0.3 μm alumina particles at radius 1.7" on disk surface

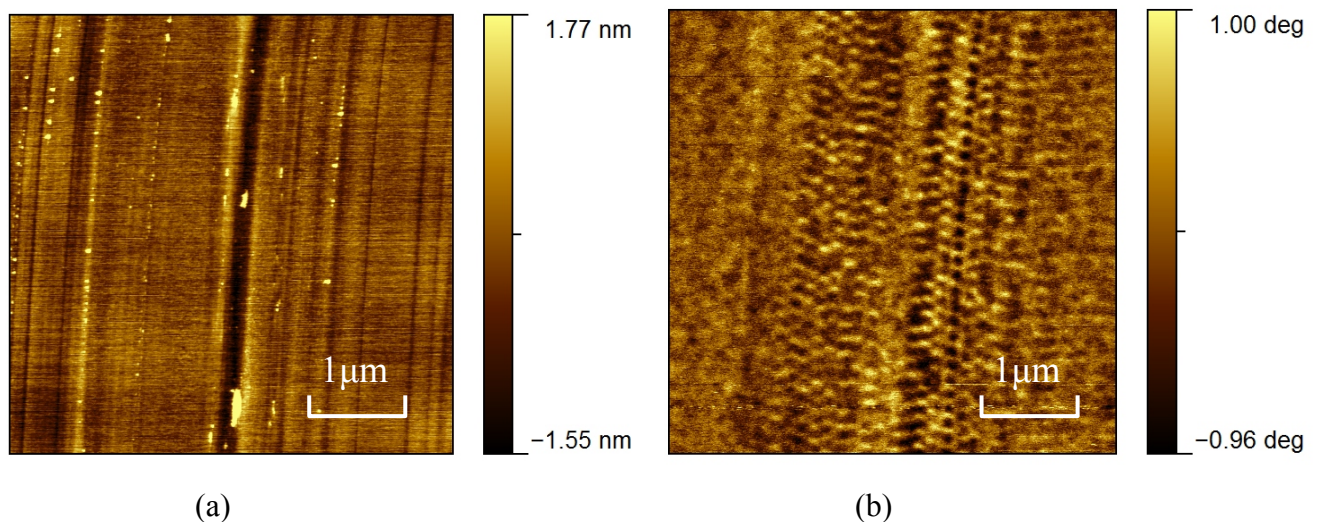


Fig.7 AFM and MFM images after sweeping experiments of 0.3 μm alumina particles between radii of 1.5" and 1.0" on the disk surface

Fig.7 shows AFM and MFM images of the disk surface after the sweeping experiments of alumina particles. Multiple scratches were found on the disk surface with maximum depth of 1.55 nm. Tiny pieces of chips were also found on the disk surface in Fig.7 (a), but they are different from what is seen in Fig.6 (a); they appear with noticeable scratches. Most of the scratches seen in Fig.7 (a) induced demagnetization except some of the scratches on the right hand side of the widest scratch in the center. It can be concluded that particle caused scratches was the major disk damage pattern in the sweeping experiment.

In Fig.6 and Fig.7 the maximum depth of the scratches caused by the alumina particles are around 1.5 nm, which is 2 nm less than the threshold value to cause demagnetization suggested by Furukawa [5]. In Fig.6, the fact that the width of the demagnetized area is larger than the scratches themselves suggests that plastic-deformation-caused grain tilt is not the only mechanism that accounts for demagnetization. In this study the disks were running at a speed of 5400 RPM, which is much faster than the reported 0.1 mm/s in Masaru' s experiments. At these higher speeds either particle scratching or rolling is able to generate considerable heat flux, which could be large enough to heat the recording layer up to or beyond its flash temperature. Therefore heat is the other mechanism that can account for demagnetization and can compensate the 2 nm gap to the threshold value.

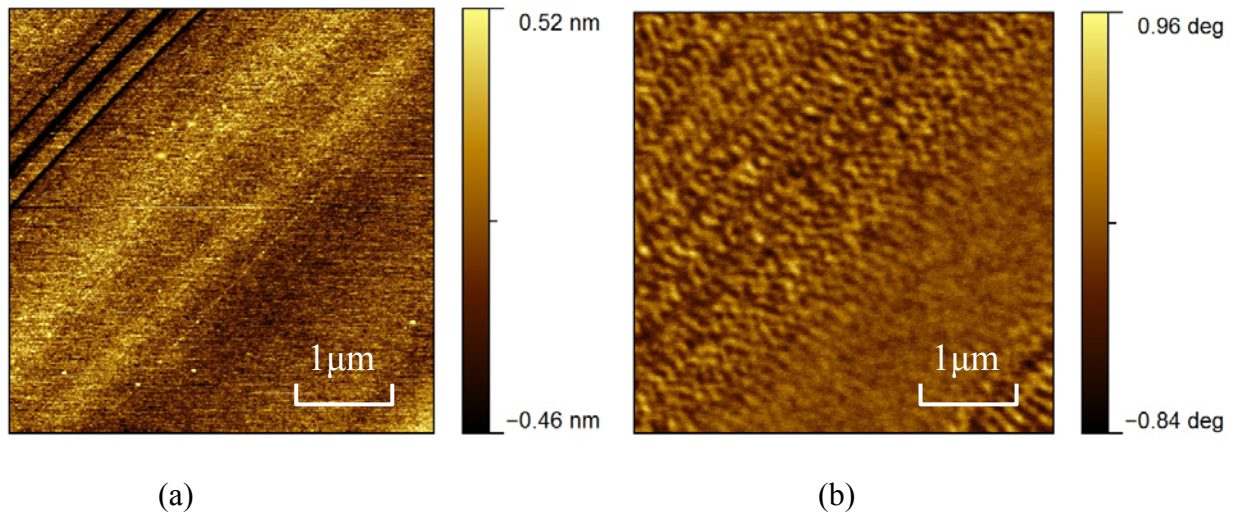


Fig.8 AFM and MFM images after fixed radius experiments with 44 μm stainless steel particles at radius 1.7" on disk surface

In the stainless steel particle experiments, fewer scratches were detected than in the alumina particle experiments, but it does not mean that these particles have less capability to cause damage to the disks. In the fixed radius experiments with stainless steel particles, as shown in Fig.8, several scratches can be seen on the upper right hand region of the AFM image, however, their depth is about 0.46 nm which is not deep enough to produce demagnetization, as seen in Fig.8 (b). A relatively large region of demagnetization was observed without any physical damage in Suk [6] and Ovcharenko [7]. Such slider-disk rubbing is also detected in Fig.3 (b), and it can be surmised that the demagnetization in Fig.8 (b) is caused by slider-disk high speed contact, which can generate enough heat to demagnetize the recording layer.

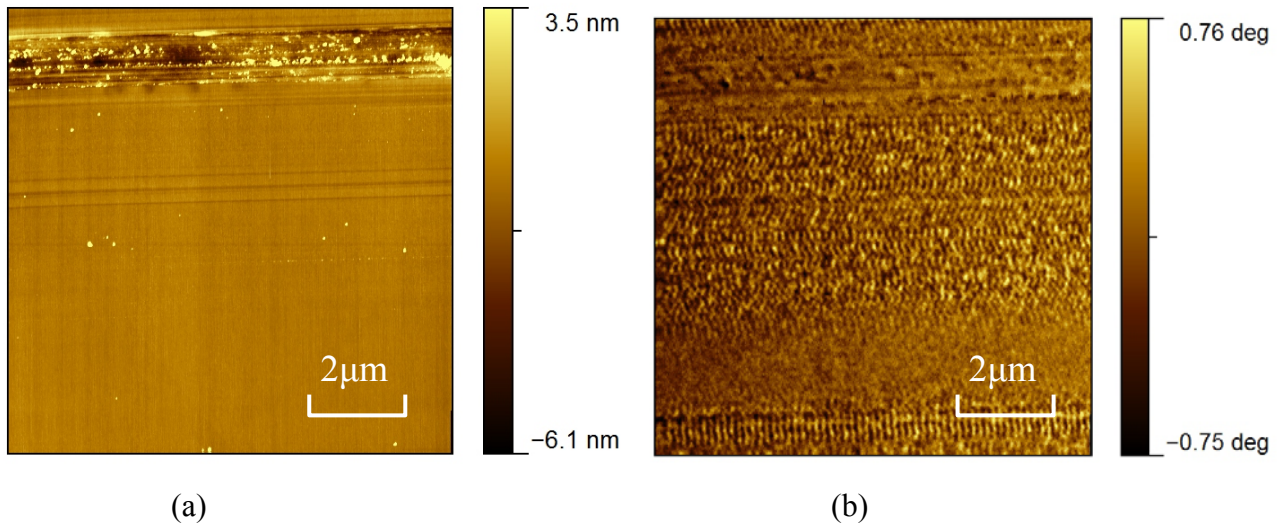


Fig.9 AFM and MFM images after sweeping experiments of 44 μm stainless steel particles between radii 1.5" and 1.0" on the disk surface

During the slider/disk contact process the slider surface can be damaged due to flying instability caused by particles, if the shearing stress exceeds the strength of the surface layer material. This kind of damage is observed on the trailing edge of the slider in the sweeping experiments of the stainless steel particles as shown in Fig.4 (b). A scratch-like damage, which consists of peelings and indentations, is seen in Fig.9 (a), causing demagnetization to the recording layer. Therefore it can be concluded that the disk layer can also be damaged from the high shearing force. The deepest part of the scratch-like damage is 6.1 nm, which already harms the recording layer directly, but the other parts of the damage was not deep enough to remove any of the recording layer. Since the demagnetized area of the scratch-like damage covers not only the deepest part but also all other shallow parts, it can be concluded that high temperature from high-speed contact contributed to the demagnetization. As in

Fig.8 (b), high-speed contact, which cannot cause physical damage, is also found in Fig.9 (b), inducing demagnetization to the recording layer. In the middle part of Fig.9 (a), scratches were also found but they are too shallow to cause any demagnetization.

3.3 DISCUSSION OF THE PARTICLE DAMAGE PATTERN

When particles are entrapped in the HDI, they can harm the slider and the disk surfaces by scratching and rolling [9]. Since the trailing edge damage is not seen in Fig.3 (a) and Fig.4 (a), high-speed slider-disk contact can be excluded from the alumina particle experiments. The apparent damage mechanism of the alumina particles is illustrated schematically in Fig.10.

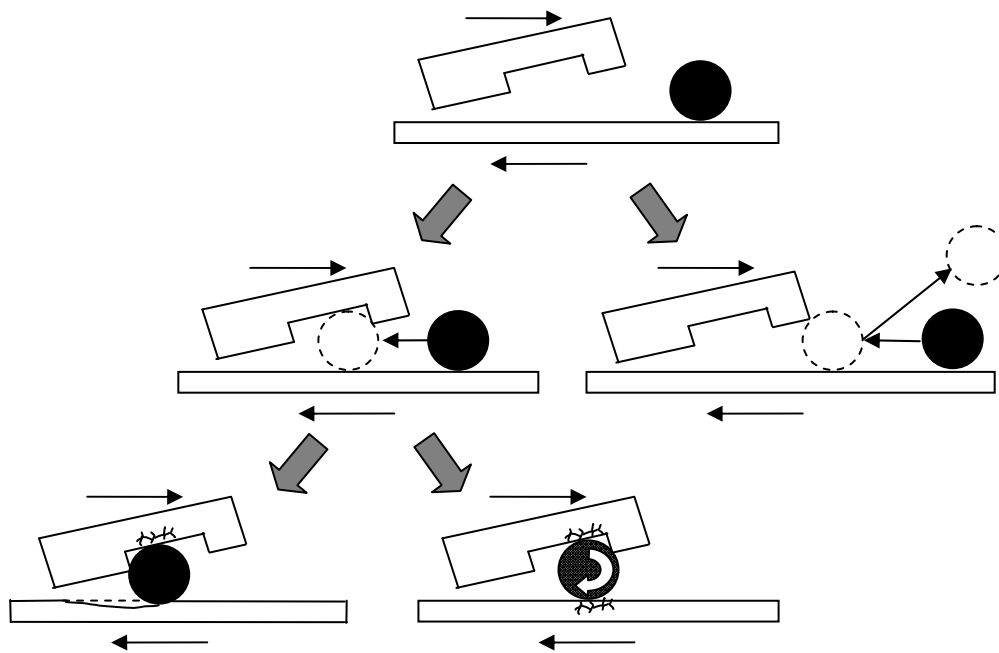


Fig.10 Schematic illustration of 0.3 μm alumina particle damage pattern

The alumina particles can be entrapped in the HDI if they find inlets on the ABS. They cause damage to both the slider and disk surfaces through

particle-slider interaction and particle-disk interaction when they are entrapped. When particles tend to scratch, a large normal force is needed to cause indentation to the slider and disk surfaces, and the entrapped particles produce considerable shearing force at the same time. The slider surface material, $\text{Al}_2\text{O}_3\text{-TiC}$, is a brittle material that cannot resist high shearing stress so that alumina particles can easily peel off the slider surface layer as shown in Fig.3 (a) and Fig.4 (a) when they are entrapped. As the top layer of the disk surface, diamond-like-carbon (DLC) has very good tribological properties to resist scratches, but it may fail at a high temperature [10], which occurs during the high-speed contact. From the experimental results, particle caused scratches were seen on the disk surface in Fig.6 and Fig.7, which are not deep but are still able to cause demagnetization. When particles are entrapped in the HDI, they also tend to roll if there is not enough normal force exerted on them. Due to the 5400 RPM disk rotating speed, considerable heat can be produced during the particle rolling process as well as sliding. For the damage seen in the bottom area of Fig.6 (a), we conclude it is high speed rolling which caused demagnetization, since the other alternative high-speed slider-disk contact was not detected in the alumina particle experiments. Besides heat, rolling particles also can cause low-cycle fatigue [11] to damage the slider and disk surfaces by producing surface micro-cracks. These micro-cracks are responsible for part of the chips found on the slider and disk surface.

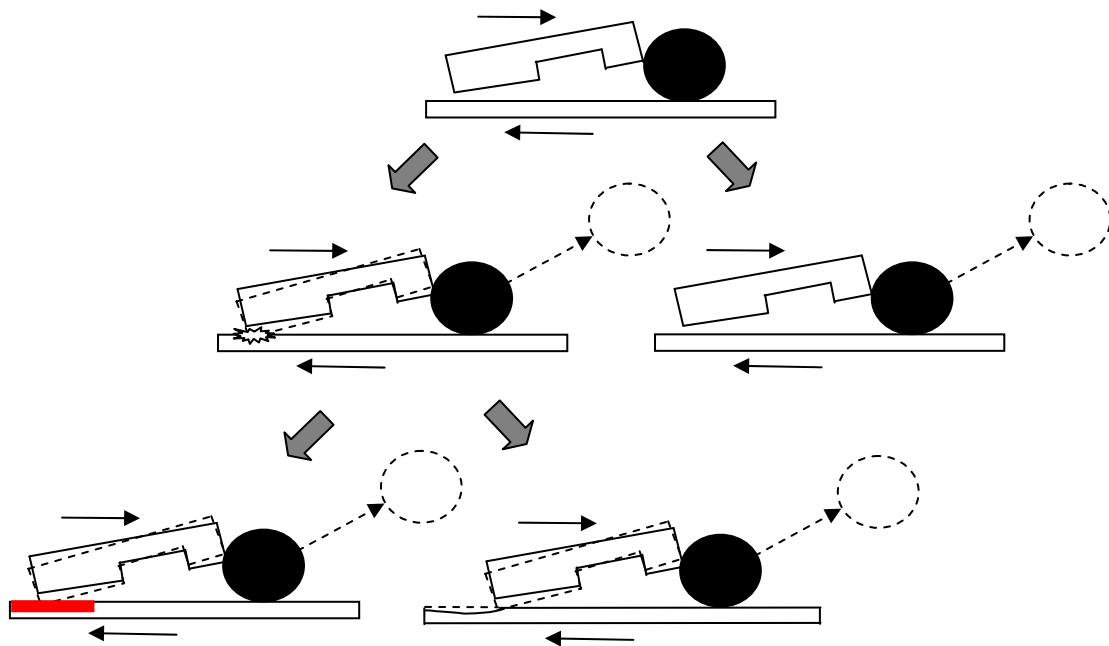


Fig.10 Schematic illustration of 44 μm stainless steel particle damage pattern

The stainless steel particles could not directly harm the slider and disk surfaces because those particles are too big for the HDI to accommodate, and they only can be swept out by the leading edge. In this case it is quite possible for them to influence the slider's flying stability because they are much larger than the alumina particles and their size is about 4.4% of the leading edge width of the pico-sliders used in these experiments. In Fig.3 and Fig.4 it can be seen that the trailing edge can be damaged from flying instability because it has the minimum flying height of the slider. The high-speed slider-disk contact not only damages the trailing edge itself but also the disk surface as shown in Fig.8 and Fig.9. High temperatures result from high-speed contact, and this is able to heat the recording layer up to or beyond its flash temperature to cause demagnetization. When the shearing stress from the contact is large enough, it can disintegrate the disk surface and result in a

rough slider trailing edge. Rough-trailing-edge to disk contact can also produce scratches according to Fig.8 and Fig.9, but the depth of these scratches is not large enough to induce any demagnetization.

4. CONCLUSION

1. 0.3 μm alumina particles get into the HDI from edge positions with the largest recess height on the ABS, and they become entrapped to cause damage to the slider and disk surfaces.
2. 44 μm stainless steel particles can be swept aside by the leading edge, but they can exert considerable counter force to influence slider's flying stability while being swept out.
3. Alumina particles scratch and roll when they are entrapped, producing both heat and plastic deformation to induce demagnetization.
4. The slider's flying stability is influenced by the larger stainless steel particles, high-speed slider-disk contact happens and produces high enough temperatures to demagnetize the recording layer. The recording layer can be directly harmed if the shearing stress is large enough during the contact.

REFERENCE:

- [1] Zhang, L., Koka, R., et al., Particle Induced Damage on Heads and Discs Due to Fine Particles of Different Materials, IEEE Transactions on Magnetics, Vol. 35, pp. 927-932, 1999.
- [2] Bhushan, B., Handbook of Micro/Nano Technology, CRC Press, pp. 505-555, 1995.
- [3] O'Brien, L., Dauber, E., et al., Controlling Disk-Drive Contamination with Adsorbent-Material Technology, Microcontamination, Vol. 12(5), pp. 31-35, 1994.
- [4] Altshuler, K., Harrison, J., et al., The Physical Effects of Intra-Drive Particulate Contamination on the Head-Disk Interface in Magnetic Hard Disk Drives, Transactions of the ASME, Vol. 121, pp. 352-358, 1999.
- [5] Furukawa, M., Xu, J., et al., Scratch-induced Demagnetization of Perpendicular Magnetic Disk, IEEE Transactions on Magnetics, Vol. 44, pp. 3633–3636, 2008.
- [6] Suk, M., Denning, P., et al., Magnetic Erasures due to Impact Induced Interfacial Heating and Magnetostriction, ASME Journal of Tribology, Vol.122, pp. 264–268, 2000.
- [7] Ovcharenko, A., Yang, M., Simulation of Magnetic Erasure Due to Transient Slider-Disk Contacts, IEEE Transactions on Magnetics, Vol. 46, pp. 770-777, 2010.
- [8] Roy, M., Brand, J., Soft Particle-Induced Magnetic Erasure Without

Physical Damage to the Media, Journal of Tribology, Vol. 129, pp. 729-734, 2007.

[9] Shen, X., Bogy. D., Contact Force and Frictional Heating due to “Large” Particles in the Head Disk Interface, Journal of Tribology, Vol. 130(1), pp. 011015.1-011015.7, 2008.

[10] Lee, K., Wei, R., Tribological Characteristics of DLC-Coated Alumina at High Temperatures, Journal of Tribology, Vol. 128(4), pp. 711-718, 2006.

[11] Fang, L., Liu, W., et al., Predicting Three-body Abrasive Wear Using Monte Carlo Methods, Wear, Vol. 256(7-8), pp. 685-694, 2004